Giant Planet Disruptions and their Effect on their Host Stars

James Guillochon
UC Santa Cruz

Abstract: Driven by dynamical processes shortly after the protoplanetary disk dissipates, giant planets can often find themselves on orbits that approach so close to their parent stars that they are disrupted. Prior work has only focused on a planet's first passage. We present 3D hydrodynamical simulations of giant planet disruptions that occur over several orbits. The inclusion of these events greatly increases the amount of mass acquired by the host stars from planetary disruptions, and can produce the observed mis-alignment between the star's rotation axis and remaining planets within the system.

Much of the planet's mass is ejected from the system completely

The planet's core can survive many orbits after the first passage

A virialized envelope of material forms via re-accretion onto the surviving core

A standing shock forms where the accretion disk and stream intersect

Approximately half of the material removed from the planet on each orbit collects in an accretion disk about the star

Figure 3. The double rainbow curves show orbital trajectories for both the planet (left) and star (right) during the encounter for different values of the periastron distance r_p. The star's trajectory is magnified by a factor of $M_*/M_P = 10^3$ to make its motion apparent. While the orbits do precess slightly over the course of the simulations, this plot shows the orbits with the precession removed. Note that the $r_p = 2.1$ run (light green) experiences a particularly ejective encounter on its 2nd periastron passage.

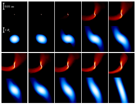

Figure 4. Slices through the orbital plane shortly after each periastron passage for the simulation where $r_p = 2.7r_t$. All plots show log ρ. The upper, red color-coded figures show a wide view of each encounter, with white corresponding to $\rho = 10^{-2}$ g cm^{-3} and black corresponding to $\rho = 10^{-7}$ g cm^{-3}, while the lower, blue color-coded figures show a close-up view of the core, with white corresponding to the maximum density ρ_{max} and black corresponding to $\rho = 10^{-2}$ g cm^{-3}.

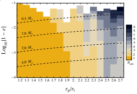

Figure 6. Criteria leading to planet ejection given an initial periastron passage distance r_p and eccentricity e. The colored regions correspond to the number of orbits before a planet is ejected by its interaction with the parent star. The dashed lines show the value of e given an apocenter distance equal to the ice line a_{ice}, assuming that $L_* \propto M_*^{3.9}$. For all values of r_p shown and for $e \lesssim 0.97$, planets are ejected before they are totally disrupted.

Table 1

Planet	r_p/r_t	$r_{a,max}/a_{ice}$	$Q_{*,max}$[a]	$\tau_{life,max}$[a] (Gyr)
HAT-P-12 b	5.2	0.41	$1\times10^4 - 1\times10^5$	0.4 — 4
OGLE-TR-56 b	4.8	0.029	$2\times10^7 - 4\times10^7$	0.9 — 2
WASP-4 b	5.1	0.093	$5\times10^7 - 2\times10^8$	1 — 6
WASP-12 b	4.7	0.021	$5\times10^7 - 2\times10^8$	0.5 — 1
WASP-19 b	3.5	0.010	$2\times10^7 - 2\times10^8$	0.07 — 1

[a] Assuming $r_{p,0} = 2r_\tau$, $a_0 = a_{ice}$. The minimum and maximum values are calculated using the lower and upper limits for τ_{age} as compiled by Schlaufman et. al 2010.

For more details, see Guillochon et. al 2010 (arXiv: 1012.2382)

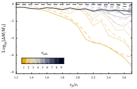

Figure 1. Mass loss history of multiple passage encounters for different initial values of r_p. Each curve is color-coded to correspond to a particular orbit number. The solid lines show the aggregate mass accreted by the star, while the dashed lines show the total mass lost from the planet.

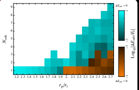

Figure 2. Change in orbital energy E_{orb} attributed to each passage as a function of r_p and orbit number N_{orb}. The orange regions show decreases in E_{orb} (more bound), while the cyan regions show increases in E_{orb} (less bound). The height of each column shows the number of orbits a planet survives before being destroyed.

$$\Delta M_*(0.37 \leq \beta \leq 0.83) = \begin{cases} 1.26 \exp\left[-0.79\beta^{-1}\right] M_J & : a_0 \ll a_{ice} \\ 9.62 \exp\left[-2.59\beta^{-1}\right] M_J & : a_0 \sim a_{ice} \end{cases} \quad (1)$$

A fit to the expected amount of mass that remains bound to the star after a multi-orbit disruption of a Jupiter-mass planet, where $\beta \equiv R_P (M_*/M_P)^{1/3}$. If the planet is scattered from the ice line (a_{ice}), its orbital energy is so small that the planet becomes unbound as soon as $\Delta E_{orb} > 0$ (see Figure 2), meaning the planet is ejected from the system prior to being completely destroyed. However, if the planet is scattered in from a distance where $E_{orb} \sim GM_P^2/R_P^2$, the planet is destroyed prior to being ejected, and up to 40% of the planet's initial mass remains bound to the star.

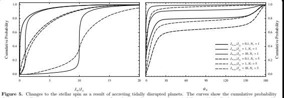

Figure 5. Changes to the stellar spin as a result of accreting tidally disrupted planets. The curves show the cumulative probability that a star will possess a given angular momentum J_* and spin inclination ψ_* after 1 (solid) or 5 (dashed) planetary disruptions N_d for different initial stellar angular momentum $J_{*,init}$, with the amount of mass accreted ΔM_* being determined from an interpolation of Figure 1. Planets are assumed to have a logarithmic distribution in mass ($0.1M_J \leq M \leq 10M_J$) and semi-major axes ($r_\tau \leq a \leq 10a_{ice}$), where r_τ is the minimum distance for which a planet won't be tidally disrupted and a_{ice} is the ice line. The eccentricity e and inclination i relative to the invariable plane are assumed to follow Rayleigh distributions, with $\sigma_e = 0.3$ and $\sigma_i = 10°$.

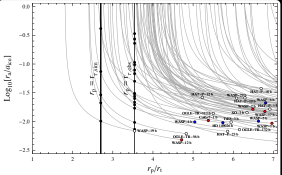

Figure 7. Possible apastrons r_a for the known hot Jupiters with $M_P > 0.1M_J$. Each arc shows the apocenter of an orbit with pericenter r_p, assuming that the angular momentum of the initial orbit is equal to the orbital angular momentum observed today. The open circles show each planet's currently observed r_p and r_a, scaled to the tidal radius r_t and the ice line a_{ice} respectively, which are determined by the planet/host star properties. Blue-filled circles are planets that are thought to be aligned with their host stars, red-filled circles are thought to be misaligned, and white-filled circles show systems with unknown orientations. The thick vertical line (labeled $r_{\tau,sim}$) shows the minimum possible value of r_τ corresponding to the Jupiter exclusion zone, which is determined through our numerical simulations for Jupiter-like planets to be $2.7r_t$, while the thinner vertical line (labeled $r_{\tau,obs}$) shows the maximum possible value for r_τ, which is defined by the planet that is currently observed to be closest to its classically defined tidal radius, WASP-19 b. Filled black circles show the intersection between the r_τ lines and each of the arcs of constant angular momentum shows the maximum apastron distance $r_{a,max}$ a planet could have been scattered from without being destroyed on its subsequent encounters with the host star. Note that the typical $r_{a,max}$ values are significantly smaller than a_{ice}, which indicates that those planets must have migrated prior to being scattered if planet-planet scattering brought them to their current positions.

As the planet is likely to be tidally locked even prior to circularization, the timescale for evolution of the planet's semi-major axis is entirely determined by the star's properties and the orbital frequency ω (Dobbs-Dixon et. al 2004),

$$\frac{a}{\dot{a}} = \frac{1}{9} Q_* \left(\frac{M_*}{M_P}\right)\left(\frac{a}{R_*}\right)^5 (\omega - \Omega_*)^{-1}, \quad (2)$$

where R_* is the star's radius, Q_* is the star's tidal quality factor, and Ω_* is its rotation frequency. The fastest inward migration occurs when a star is not rotating, e.g. $\Omega_* \to 0$. As planet-planet scattering seems to be rare after 10^8 yr (Matsumura et. al 2008), we can set $a/\dot{a}$ equal to the system age τ_{age} to determine $Q_{*,max}$, the maximum tidal quality factor for which a planet can migrate from $2r_\tau$ to a_{obs}

$$Q_{*,max} = 7\times10^5 \left(\frac{M_P}{M_J}\right)^{8/3}\left(\frac{M_*}{M_\odot}\right)^{-8/3}\left(\frac{R_P}{R_J}\right)^{-5}\left(\frac{r_\tau}{3r_t}\right)^{-5}\left(\frac{P_0}{3\ \mathrm{days}}\right)^{-1}\left(\frac{\tau_{age}}{\mathrm{Gyr}}\right) \quad (3)$$

where P_0 is the initial orbital period. When setting $r_\tau = r_{\tau,sim}$, all of the known hot Jupiters with $a_{obs} < 2r_\tau$ yields values for $Q_{*,max}$ that are consistent with those expected for stars (Table 1).